JOURNAL OF APPLIED PHYSICS **101**, 114507 (2007)

High-frequency surface acoustic wave devices based on AlN/diamond layered structure realized using e-beam lithography

M. B. Assouar,[a)] O. Elmazria, P. Kirsch, and P. Alnot
Laboratoire de Physique des Milieux Ionisés et Applications, Nancy-University – CNRS, 54506 Vandoeuvre-lès-Nancy, France

V. Mortet
Institute for Materials Research-Limburgs Universitair Centrum, Wetenschapspark 1-B-3590 Diepenbeek, Belgium

C. Tiusan
Laboratoire de Physique des Matériaux, Nancy-University – CNRS, 54506 Vandoeuvre-lès-Nancy, France

(Received 15 January 2007; accepted 6 April 2007; published online 12 June 2007)

We report in this paper on the study and the realization of surface acoustic wave devices based on an AlN/diamond layered structure intended for the X band (8 GHz). Both x-ray diffraction and transmission electronic microscopy, used for characterization of the structural properties of the AlN/diamond structure, have shown (002) highly oriented sputtered AlN films on free-standing chemical vapor deposition diamond films. Surface roughness of the AlN/diamond structure was measured by atomic force microscopy and showed a very low surface roughness, less than 1 nm. Low surface roughness is very important to reduce the acoustic propagation losses. SAW devices operating in the range of 8 GHz were realized by the combination of the high velocity of the AlN/diamond layered structure and the high lateral resolution obtained using e-beam lithography (EBL). Due to high electrical resistivity of the AlN film, interdigital transducers with submicronic resolution were patterned by an adapted technological EBL process. The analysis of device performances in terms of electromechanical coupling coefficient and temperature stability was carried out and discussed. The dispersion of both parameters as a function of wavelength was experimentally determined, and showed the obtention of an electromechanical coupling coefficient up to 1.4% and a temperature coefficient of frequency varying between 9 and 20 ppm/°C. The dispersion curves of phase velocity were also analyzed and experimental results show a good agreement with theoretical calculations. © *2007 American Institute of Physics*.
[DOI: 10.1063/1.2739218]

I. INTRODUCTION

Surface acoustic waves have been applied in various electronic and communication systems. Recently, surface acoustic wave (SAW) devices, which process signals in a very simple form, have been expected to be applied in X band mobile communication systems, and research is done to expand their operating frequencies from ultrahigh frequency (UHF) to the X band. The SAW devices operating frequency is given by the following equation: $f=V/\lambda$, where V is the phase velocity and λ is the wavelength corresponding to the period of the interdigital transducers (IDTs). There are different approaches to achieve higher-frequency operation: reducing the period of IDTs, using a substrate with higher propagation velocity, using leaky SAW, etc.[1] Until now, only studies on increasing operating frequency by using diamond film or by reducing the IDT lateral resolution were done.[2,3] In this study, and in order to realize SAW devices for X band, the first approaches are combined: the use of diamond as high velocity substrate and the e-beam lithography for achieving high lateral resolution of IDTs.

Polycrystalline diamond has attracted considerable interest in recent years for the fabrication of SAW devices as the elastic constant of diamond is the highest of all available materials, resulting in a SAW velocity of about 12 000 m/s.[4–6] For this reason, and although diamond is not piezoelectric, it is a desirable substrate for SAW devices when combined with piezoelectric thin films such as aluminum nitride (AlN)[7–9] or zinc oxide (ZnO).[2,10] The AlN/diamond structure has the advantage of having a smaller velocity dispersion compared to the ZnO/diamond structure, because the difference in phase velocity between AlN and diamond is smaller than that between ZnO and diamond.[11] On the other hand, e-beam lithography (EBL) is one of the most versatile techniques for the fabrication of submicrometer and nanometric structures.[12,13] We use e-beam to develop high lateral resolution IDTs in order to decrease the wavelength, inducing an increase of the SAW devices' operating frequency.

II. EXPERIMENTAL

A. CVD diamond deposition

Polycrystalline diamond films were grown on silicon wafers by plasma-enhanced chemical vapor deposition (PECVD) using an ASTeX reactor. The details of diamond substrate growth are given elsewhere.[4] After deposition, the

a)Electronic mail: badreddine.assouar@lpmi.uhp-nancy.fr

 © 2007 American Institute of Physics

Downloaded 11 Feb 2008 to 194.214.217.17. Redistribution subject to AIP license or copyright; see http://jap.aip.org/jap/copyright.jsp

polycrystalline diamond layer was removed from the silicon substrate by a wet chemical etching in a HNA solution ($HF:HNO_3:CH_3COOH$), leading to a free-standing diamond layer with a flat surface on the nucleation side. The nucleation side of the free-standing diamond surface is smooth, with an average root-mean-square (rms) roughness R_{rms} of about 1 nm. In fact, this low roughness value is achieved due to the use of a bias-enhanced nucleation technique for diamond layer growth.[8,14] The free-standing CVD diamond layers were chemically oxidized in a hot $CrO_3:H_2SO_4$ solution and organically cleaned prior to the deposition of AlN thin films. In this crucial step, any nondiamond carbon, which might be present from the initial stage of deposition, is removed. In this way, a suitable surface for preparation of the (002) oriented AlN films is obtained.

B. AlN deposition

The AlN films were deposited by reactive RF magnetron sputtering on the free-standing CVD diamond layer. The process deposition of AlN films on silicon substrates was published elsewhere,[15] and shows the obtaining of highly oriented AlN films on silicon substrates. Concerning free-standing diamond layers, a few optimizations of AlN film deposition were carried out in order to obtain the high (002) orientation. In fact, the lattice parameter of AlN is closer to that of diamond than to that of silicon. The lattice mismatch between AlN and silicon is 0.74, compared to 0.14 for AlN and diamond. With regard to this fact, we understand clearly that we can obtain a highly oriented AlN film on a diamond layer.

C. e-beam

e-beam lithography was used to pattern the interdigital transducers on AlN/diamond layered structure. Because of the high resistivity of this structure, it is very difficult to develop a pattern due to the electrons' accumulation on the structure's surface. To overcome this problem, an adapted technological process was pointed out enabling the realization of a nonsymmetrical pattern on highly resistive materials.[16] Then, the IDTs made in aluminum with resolutions down to 250 nm were successfully patterned on AlN/diamond layered structure with this adapted technological process. The length and the thickness of IDTs are, respectively, 100 μm and 100 nm.

III. RESULTS AND DISCUSSION

First of all, we started with the characterizations of materials composing the layered structure. Then, the characterizations of structural properties of AlN films deposited on diamond layer were carried out using x-ray diffraction (XRD) and transmission electronic microscope (TEM) analysis. Figure 1 shows the XRD spectrum in a $\theta/2\theta$ scan mode of the AlN film deposited on the nucleation side of the CVD diamond substrate. One can observe that the AlN film is highly oriented on (002), corresponding to the c axis perpendicular to the surface. We can also observe the peaks corresponding to (111) and (220) CVD diamond orientations, which indicate that the diamond substrate presents two preferential orientations. The rocking curve on the AlN (002) diffraction has also been measured in order to evaluate the misaligned columns of AlN films. Figure 2 shows a Gaussian shape of the rocking curve made on the (002) diffraction peak of the AlN/diamond layered structure. The full width at half-maximum (FWHM) of this curve, which gives the degree of (002) AlN film orientation, is 1.67°. This FWHM value is very low considering that the AlN films were deposited by magnetron sputtering, and attests to the high crystalline quality of AlN films deposited on free-standing CVD diamond.

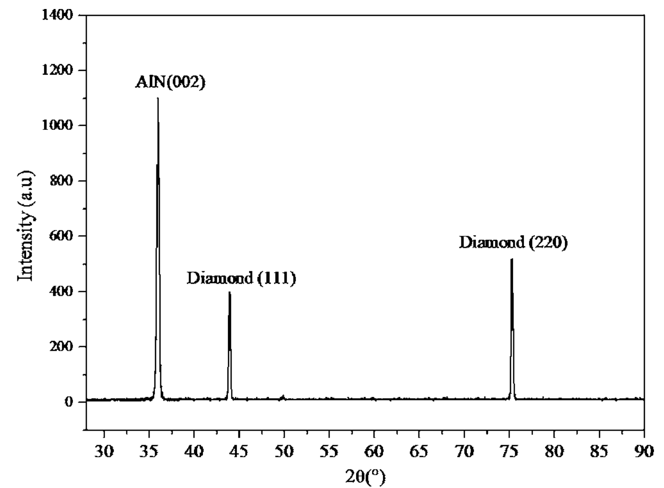

FIG. 1. X-ray diffraction of AlN/diamond layered structure.

In order to investigate the microstructure of the AlN film deposited on the diamond layer, TEM analysis was used. Figure 3 shows a TEM plane view of AlN film, which exhibits clearly a very small grain size. This observation is very important in order to have an idea about the surface roughness of the AlN/diamond layered structure. In fact, the grain size of the film is linked to its surface roughness, and the roughness is a very crucial parameter that has a great effect on surface acoustic wave propagation and notably on acoustic losses in high-frequency SAW devices. In fact, with increasing frequency, the penetration depth of SAWs in the layered structure becomes smaller and should be more af-

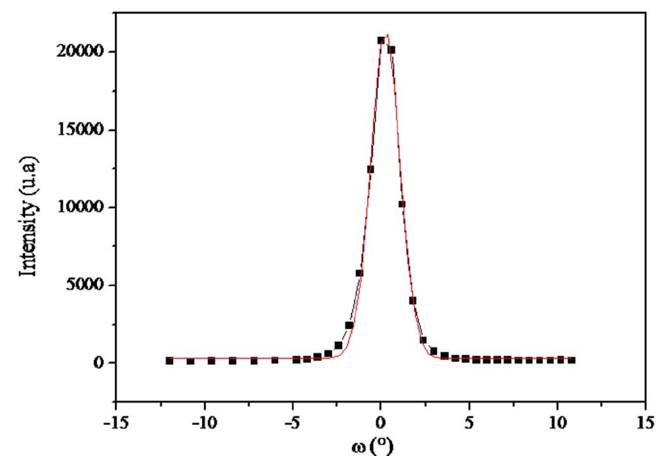

FIG. 2. Rocking curve of (002) AlN film orientation indicating a FWHM value of 1.67°.

Downloaded 11 Feb 2008 to 194.214.217.17. Redistribution subject to AIP license or copyright; see http://jap.aip.org/jap/copyright.jsp

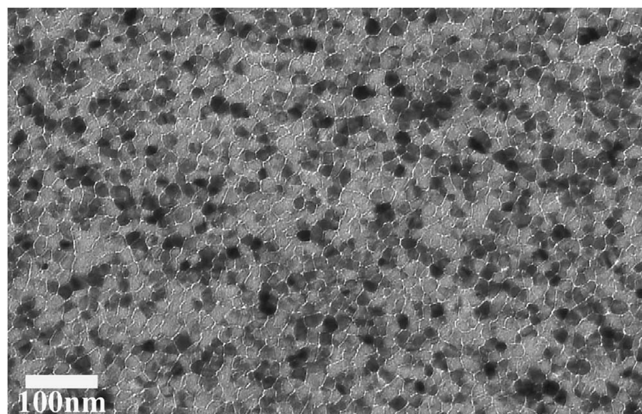

FIG. 3. Plane view of transmission electron microscope image shows the microstructure and grain size of AlN thin film.

fected by roughness, inducing scattering and attenuation of the waves.[17] From Fig. 3, the grain size of AlN film was estimated to be about 20 nm, which can induce a very low surface roughness. In this view, we have realized a surface roughness measurement using atomic force microscopy (AFM). Figure 4 shows a three-dimensional (3D) AFM image of the AlN surface film deposited on the nucleation side of the free-standing diamond layer. One can observe that the surface is very flat and the surface roughness ($R_{\rm rms}$) is less than 1 nm, which is very important and very suitable to reduce the propagation losses of surface acoustic waves, particularly at the high frequency range.

After the thin films' structural and morphological characterizations, several SAW devices with submicrometer features were realized by the technological process described previously. SAW devices with various spatial periodicities (wavelengths) from 1 to 3.2 μm with a step size of 0.2 μm have been realized. The corresponding finger widths vary from 250 to 800 nm. For all these devices, the aperture is fixed to 90 μm and the gap between the IDT emitter and receiver is fixed to 20 μm, except for the device with the lowest spatial resolution of 250 nm, where the gap is fixed to 10 μm and the aperture is fixed to 80 μm. Each IDT consists of 50 pairs of fingers, except for the IDTs with 250 nm lateral resolution, which have 75 finger pairs.

We have proceeded to the frequency characterization of the obtained SAW devices, using an Agilent 8752A network

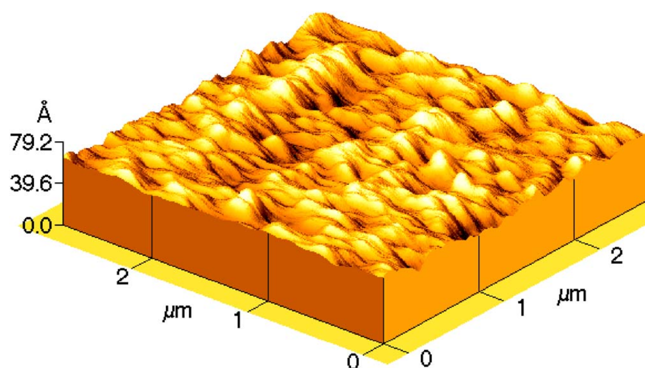

FIG. 4. Atomic force microscope 3D image of AlN film surface (3 μm $\times 3$ μm) exhibiting very low roughness.

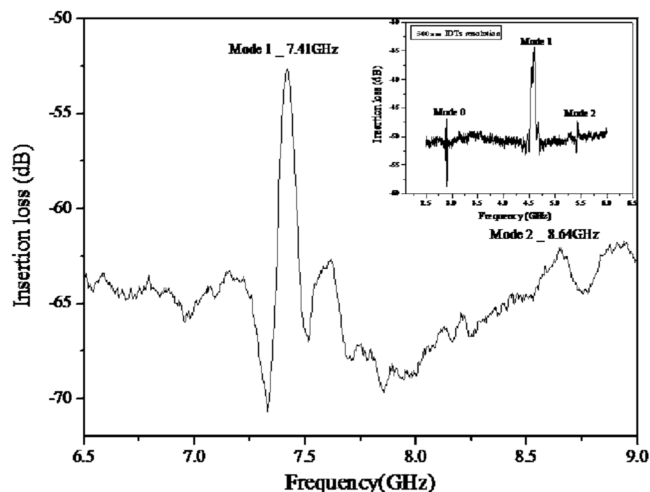

FIG. 5. Frequency response of SAW device based on AlN/diamond layered structure with 250 nm IDTs lateral resolution. Inset, the SAW device frequency response achieved with 500 nm IDTs lateral resolution.

analyzer and a RF microprober (Suss Microtech). The thickness of AlN film used for all realized SAW structures is 1 μm. Figure 5 presents the frequency response of the SAW device with IDT lateral resolution of 250 nm. This means that the wavelength is 1 μm and the normalized thickness kh is 6.28, where k is the wave vector and h is the AlN film thickness. One can observe that we have two modes, mode 1 at 7.41 GHz and mode 2 at 8.64 GHz, which correspond, respectively, to 7410 and 8640 m/s phase velocities, taking into account the wavelength value of 1 μm. There are two observations that we can explain here. The first one is the obtained low velocities values, which we can explain by the fact that most of the surface acoustic wave energy is confined in the 1 μm AlN film due to the low lateral resolution of IDTs, which induces a low wavelength. When the lateral resolution increases, as we can see in the inset Fig. 5, which exhibits the frequency response of the device realized with a 2 μm wavelength, the phase velocities increase due to the better penetration of surface waves into the diamond substrate. In fact, the phase velocities of modes 1 and 2 for this last device are, respectively, 9200 and 10 850 m/s. The second observation is that we cannot find the peak of mode 0. In fact, with regard to the theoretical velocity dispersion curve (Fig. 6, continuous lines) for the AlN/diamond layered structure, we should observe this slow mode. The absence of this mode can be explained by the low value of the electromechanical coupling coefficient related to it,[8] and by the increase of the propagation losses with the increasing frequency, which induces a reduction in the signal-to-noise ratio. This also explains why the characteristics, insertion loss, and the suppression level, corresponding to mode 1, exhibit lower quality for this device than for the device operating at 4.5 GHz (Fig. 5, inset). In Fig. 6, the continuous lines represent the theoretical values and the dots represent the experimental ones obtained from all realized SAW devices in this study. One can observe that we have a very good agreement between experimental and calculated values.

Concerning the electrical performances of the realized devices, we observe a relatively high insertion loss consider-

Downloaded 11 Feb 2008 to 194.214.217.17. Redistribution subject to AIP license or copyright; see http://jap.aip.org/jap/copyright.jsp

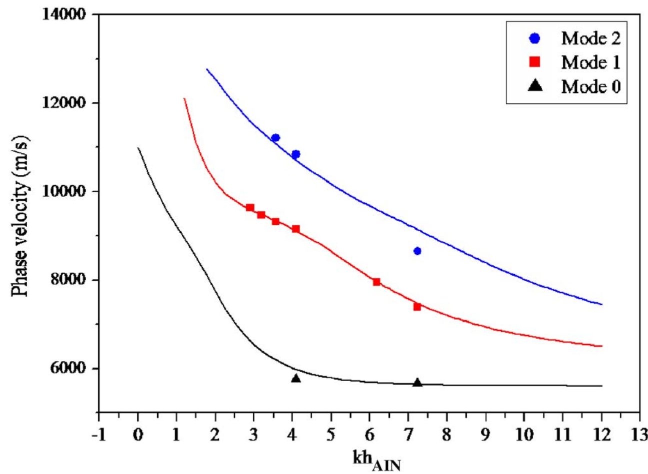

FIG. 6. Experimental (dots) and calculated (lines) phase velocity dispersion curve relative to achieved SAW devices.

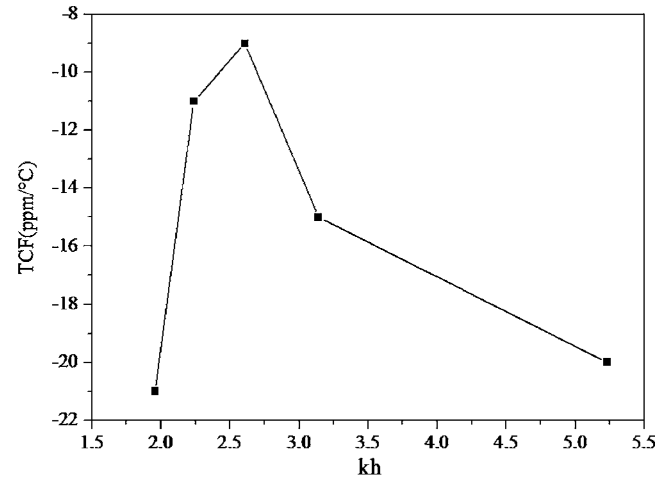

FIG. 8. Experimental dispersion curve of temperature coefficient of frequency determined in the range of 20–100 °C.

ing the frequency responses. This is due to many reasons. The first one is the acoustic losses and diffusion due to the low roughness of realized aluminum IDTs. In fact, at high lateral resolutions, the development of IDTs by EBL combined with the lift-off process induces a small roughness of the IDTs fingers due to the aluminum deposition process. The second reason is relative to the IDTs design. In fact, no particular IDT design was used in our SAW devices to reduce the insertion loss. Indeed, the relative high insertion loss observed for SAW frequency response was expected.

The achieved SAW devices were characterized in terms of electromechanical coupling, and in terms of temperature stability to evaluate the temperature effect on SAW devices operating at high frequencies. We have carried out the measurements of the electromechanical coupling coefficient (K^2) of all realized SAW devices with various lateral IDT resolutions (250–800 nm). The measurements were done based on the mode 1 peak. Figure 7 shows the measured and theoretical K^2 values as a function of the normalized thickness kh. Concerning the experimental values, one can see that the K^2 increases with decreasing wavelength, and tends to stabilize at a kh of 3, which corresponds to a wavelength of 2 μm.

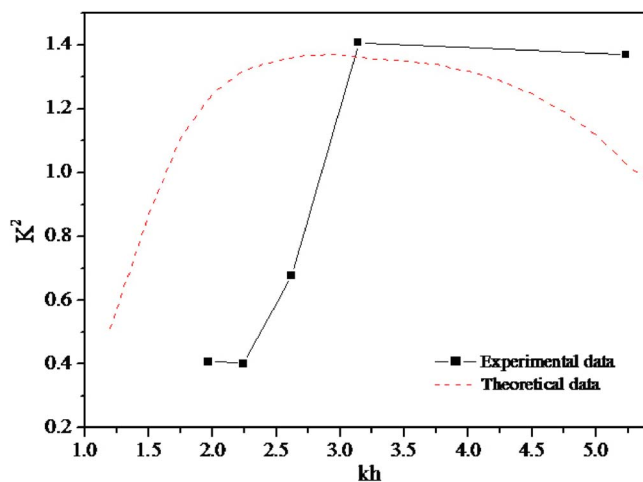

FIG. 7. Experimental (black dots) and calculated (dashed line) electromechanical coupling coefficient dispersion curves of realized SAW devices.

The trend of K^2 agrees quite well with the calculated dispersion curve, and means that we have to set the normalized thickness at a value of 3 in order to obtain the best electrical performances of our SAW devices. This thickness will also increase the phase velocity of the AlN/diamond structure.

The difference between theoretical and experimental values of K^2 can be explained by the fact that in the theoretical calculations, we do not take into account the mass loading effects of aluminum thickness. In experimental approaches, this effect is observed and the increase of K^2 is due also to the aluminum grating, which operates as a resonator.

Concerning the temperature stability of SAW devices, we have measured the operating frequency shift in the range of 20–100 °C for each device, which gives the temperature coefficient of frequency (TCF), the parameter indicating the SAW devices' temperature stability. Note that a low value of TCF is desired and the conventional piezoelectric materials such as $LiNbO_3$ show a TCF value in the range of 70 ppm/°C. Figure 8 shows the TCF dispersion versus normalized thickness kh. One can observe that the TCF increases in the kh range between 2 and 3, exhibiting a value between −21 and −9 ppm/°C. In this range, the wavelength decreases, meaning that the acoustic waves are more confined in the AlN film, and consequently the TCF of AlN film, which is positive,[18] and the TCF of diamond layer, which is negative,[19,20] affects more the TCF of AlN/diamond layered structure. However, in the kh range between 3 and 5.24, the measured TCF decreases from −9 to −20 ppm/°C. This behavior is very surprising knowing that AlN and diamond exhibit opposite signs of TCF. In fact, the TCF is expected to increase with the kh value until zero. Note that to the best of our knowledge, no study concerning TCF dispersion on AlN/diamond layered structure exists. This is probably due to the unavailability of precise temperature elastic constants of AlN film. Furthermore, some contradictions were recorded, and we found in the literature that the TCF value of AlN film is either positive[18] or negative.[21,22] So, at the moment, the behavior of TCF of high-frequency SAW devices based on AlN/diamond layered structure remains unclear.

Downloaded 11 Feb 2008 to 194.214.217.17. Redistribution subject to AIP license or copyright; see http://jap.aip.org/jap/copyright.jsp

IV. CONCLUSION

Very high-frequency SAW devices operating at frequencies up to 8 GHz were performed on an AlN/diamond multilayer structure using e-beam lithography combined with a lift-off process. The materials' characterizations of composed layered structures were carried out, and have shown high crystalline and morphological qualities of AlN and diamond layers, crucial to realizing high-performance devices. The obtained results show the good quality of the operating SAW device achieved using the developed technological process. The lateral resolution of 250 nm was reached. The obtained frequency responses showed very interesting frequency characteristics, and pointed out the different propagation modes in agreement with the theoretical values of acoustic velocities and electromechanical coupling coefficients. The dispersion of the temperature coefficient of frequency was studied, and shows a pseudoparabolic behavior, which cannot be explained at this stage of this study, and more investigations are required. The combination of high acoustic velocity materials such as diamond and the e-beam lithography technique allows realization of SAW devices operating in the X band, with good electrical performances and relatively good temperature stability.

[1] K. Yamanouchi, N. Sakurai, and T. Satoh, Proc.-IEEE Ultrason. Symp. **1**, 351 (1989).
[2] H. Nakahata, K. Higaki, S. Fujii, A. Hachigo, H. Kitabayashi, K. Tanabe, Y. Seki, and S. Shikata, Proc.-IEEE Ultrason. Symp. 361 (1995).
[3] T. Palacios, F. Calle, E. Monroy, J. Grajal, M. Eickhoff, O. Ambacher, and C. Prieto, Mater. Sci. Eng., B **93**, 154 (2002).
[4] V. Mortet, O. Elmazria, M. Nesladek, M. B. Assouar, G. Vanhoyland, J. D'Haen, M. D'Olieslaeger, and P. Alnot, Appl. Phys. Lett. **81**, 1720 (2002).
[5] M. Pereira da Cunha, E. L. Adler, and D. C. Malocha, Proc.-IEEE Ultrason. Symp. 283 (2000).
[6] G. F. Iriarte, J. Appl. Phys. **93**, 9604 (2003).
[7] P. Kirsch, M. B. Assouar, O. Elmazria, V. Mortet, and P. Alnot, Appl. Phys. Lett. **88**, 223504 (2006).
[8] O. Elmazria, M. El Hakiki, V. Mortet, M. B. Assouar, L. Bouvot, M. Nesladek, M. Vanecek, P. Bergonzo, M. D'Olieslaeger, and P. Alnot, IEEE Trans. Ultrason. Ferroelectr. Freq. Control **51**, 1704 (2004).
[9] M. Benetti, D. Cannatà, F. Di Pietrantonio, and E. Verona, Proc.-IEEE Ultrason. Symp. 1738 (2003).
[10] A. Hachigo, H. Nakahata, K. Itakura, S. Fujii, and S. Shikata, Proc.-IEEE Ultrason. Symp. 325 (1999).
[11] G. F. Iriarte, F. Engelmark, I. V. Katardjiev, V. Plessky, and V. Yantchev, IEEE Trans. Ultrason. Ferroelectr. Freq. Control **50**, 1542 (2003).
[12] H. Hatakeyama, T. Omori, K.-Y. Hashimoto, and M. Yamaguchi, IEEE Trans. Int. Ultrason. Ferroelectr. Freq. Control Joint 50th Anniversary Conference, 1896 (2004).
[13] T. Palacios, F. Calle, E. Monroy, and E. Muñoz, J. Vac. Sci. Technol. B **20**, 2071 (2002).
[14] V. Mortet, O. Elmazria, M. Nesládek, M. Elhakiki, G. Vanhoyland, J. d'Haen, M. d'Olieslaeger, and P. Alnot, Phys. Status Solidi A **199**, 145 (2003).
[15] M. B. Assouar, M. El Hakiki, O. Elmazria, P. Alnot, and C. Tiusan, Diamond Relat. Mater. **13**, 1111 (2004).
[16] P. Kirsch, M. B. Assouar, O. Elmazria, C. Tiusan, and P. Alnot, Proc. IEEE Int. Symp. Appl. Ferroelectr. 2293 (2006).
[17] C. M. Flannery and H. Von Kiedrowski, Ultrasonics **40**, 83 (2002).
[18] T. Shiosaki, Y. Mikamura, F. Tadeka, and A. Kawabata, IEEE Trans. Ultrason. Ferroelectr. Freq. Control **33**, 324 (1986).
[19] H. Nakahata, H. Kitabayashi, S. Fujii, K. Higaki, K. Tanabe, Y. Seki, and S. Shikata, Proc.-IEEE Ultrason. Symp. 285 (1996).
[20] S. Ono, K. Wasa, and S. Hayakawa, Wave Electron. **3**, 35 (1977).
[21] M.-A. Dubois and P. Muralt, Appl. Phys. Lett. **74**, 3032 (1999).
[22] K. Nakamura, H. Sasaki, and H. Shimizu, Electron. Lett. **17**, 507 (1981).

Downloaded 11 Feb 2008 to 194.214.217.17. Redistribution subject to AIP license or copyright; see http://jap.aip.org/jap/copyright.jsp